Table 1.

Whole brain white matter parcellated into 50 white matter regions based on the ICBM young adult DTI-81 atlas (* indicates tracts that are present in both left and right hemispheres)

MCP	Middle cerebellar peduncle	BCC	Body of corpus callosum
PCT	Pontine crossing tract	SCC	Splenium of corpus callosum
ICP*	Inferior cerebellar peduncle	GCC	Genu of corpus callosum
SCP*	Superior cerebellar peduncle	ACR*	Anterior corona radiata
CST*	Corticospinal tract	ML*	Medial lemniscus
PCR*	Posterior corona radiata	PTR*	Posterior thalamic radiation
SS*	Sagittal stratum	FX	Fornix
UNC*	Uncinate fasciculus	TAP*	Tapetum
CP*	Cerebral peduncle	EC*	External capsule
ALIC*	Anterior limb of internal capsule	RLIC*	Retrolenticular part of internal capsule
PLIC*	Posterior limb of internal capsule	FX/ST*	Fornix / Stria terminalis
CGH*	Cingulum (hippocampus part)	SLF*	Superior longitudinal fasciculus
IFO*	Inferior fronto-occipital fasciculus	SFO*	Superior fronto-occipital fasciculus
SCR*	Superior corona radiata	CGC*	Cingulum (cingulate gyrus part)

Table 2.

Thirty-four Freesurfer-derived cortical labels per hemisphere extracted as the basis for our 68x68 cortical connectivity matrices used in the inter-hemispheric integration analysis (note that these do not include the additional 19 Freesurfer-derived subcortical gray matter regions).

1	Banks of the superior temporal sulcus	18	Pars orbitalis
2	Caudal anterior cingulate	19	Pars triangularis
3	Caudal middle frontal	20	Peri-calcarine
4	Cuneus	21	Postcentral
5	Entorhinal	22	Posterior cingulate
6	Fusiform	23	Pre-central
7	Inferior parietal	24	Precuneus
8	Inferior temporal	25	Rostral anterior cingulate
9	Isthmus of the cingulate	26	Rostral middle frontal
10	Lateral occipital	27	Superior frontal
11	Lateral orbitofrontal	28	Superior parietal
12	Lingual	29	Superior temporal
13	Medial orbitofrontal	30	Supra-marginal
14	Middle temporal	31	Frontal pole
15	Parahippocampal	32	Temporal pole
16	Paracentral	33	Transverse temporal
17	Pars opercularis	34	Insula

Table 3. Mean and standard deviation (SD) of global network metrics for the bipolar and healthy control subjects in this study (element-wise inverse mapping was used to calculate the characteristic path length and global efficiency)

		Value	F	df	*P*
Clustering coefficient					
	Bipolar	11.82±(1.100)			
	Healthy controls	12.59±(1.507)			
			11.0	1,44	0.002
Characteristic path Length (using element-wise inverse mapping, see text)					
	Bipolar	0.061±(0.013)			
	Healthy controls	0.055±(0.011)			
			6.57	1,44	0.014
Degree					
	Bipolar	18.77±(1.324)			
	Healthy controls	19.07±(1.197)			
			1.31	1,44	0.258
Eglobal (using element-wise inverse mapping)					
	Bipolar	33.03±(3.827)			
	Healthy controls	36.05±(4.496)			
			14.9	1,44	<0.001

Table 4. Mean and standard deviation (SD) of local node-level network metrics for the 20 fronto-limbic ROIs (10 in each hemisphere) proposed in our a priori hypotheses. Only regions exhibiting significant group differences at p=0.05 (uncorrected) are shown (the element-wise inverse mapping was used to generate node-level path length).

		Clustering Coefficient	**F**	***df***	***P***
Hippocampus, left					
	Bipolar	6.37±(1.288)			
	Healthy controls	7.54±(1.885)			
			8.10	1,44	0.007
Isthmus cingulate, right					
	Bipolar	7.84±(2.577)			
	Healthy controls	9.26±(1.947)			
			5.62	1,44	0.022

		Path Length	***F***	***df***	***P***
Hippocampus, left					
	Bipolar	0.046±(0.008)			
	Healthy controls	0.041±(0.007)			
			12.5	1,44	0.001
Hippocampus, right					
	Bipolar	0.046±(0.008)			
	Healthy controls	0.042±(0.007)			
			7.72	1,44	0.008
Caudalanterior cingulate, left					
	Bipolar	0.042±(0.008)			
	Healthy controls	0.039±(0.007)			
			4.74	1,44	0.035
Isthmus cingulate, left					
	Bipolar	0.054±(0.009)			
	Healthy controls	0.046±(0.009)			
			13.37	1,44	0.001

Lateral orbitofrontal, left					
	Bipolar	0.048±(0.008)			
	Healthy controls	0.043±(0.007)			
			10.66	1,44	0.002
Medial orbitofrontal, left					
	Bipolar	0.047±(0.008)			
	Healthy controls	0.044±(0.007)			
			6.12	1,44	0.017
Parahippocampal, left					
	Bipolar	0.109±(0.039)			
	Healthy controls	0.087±(0.031)			
			5.32	1,44	0.026
Caudalanterior cingulate,					
	Bipolar	0.041±(0.007)			
	Healthy controls	0.038±(0.007)			
			4.46	1,44	0.040
Isthmus cingulate, right					
	Bipolar	0.051±(0.008)			
	Healthy controls	0.042±(0.008)			
			23.8	1,44	<0.001
Lateral orbitofrontal, right					
	Bipolar	0.049±(0.008)			
	Healthy controls	0.045±(0.008)			
			7.51	1,44	0.009
Medial orbitofrontal, right					
	Bipolar	0.045±(0.007)			
	Healthy controls	0.042±(0.008)			
			5.88	1,44	0.02

Table 5. Post-hoc analyses of inter-hemispheric integration in the frontal, temporal, parietal, and occipital lobes. This table shows the mean and standard deviation (SD) of lobar inter-hemispheric path length and efficiency (computed using both connectivity-to-length mappings). Only group differences reaching statistical significance are shown (Bonferroni correction with a total of 16 tests; cut-off p value 0.05/16=0.003)

Element-wise inverse mapping			***F***	***df***	***P***
Inter-hemispheric path length Occipital lobe					
	Bipolar	0.054±(0.014)			
	Healthy controls	0.044±(0.010)			
			10.64	1,44	0.0021
Inter-hemispheric efficiency Frontal lobe					
	Bipolar	22.9±(4.86)			
	Healthy controls	27.9±(6.26)			
			17.29	1,44	1.5×10^{-4}
Inter-hemispheric efficiency Temporal lobe					
	Bipolar	54.6±(17.9)			
	Healthy controls	71.4±(20.3)			
			11.27	1,44	0.0016
Inter-hemispheric efficiency Occipital lobe					
	Bipolar	22.9±(4.86)			
	Healthy controls	27.9±(6.26)			
			10.38	1,44	0.0024
Inter-hemispheric efficiency Parietal lobe					
	Bipolar	54.6±(17.9)			
	Healthy controls	71.4±(20.3)			
			9.87	1,44	0.0030

Element-wise inverse square root mapping			***F***	***df***	***P***
Inter-hemispheric path length Frontal lobe					
	Bipolar	0.40±(0.044)			
	Healthy controls	0.37±(0.037)			
			12.20	1,44	0.0011
Inter-hemispheric path length Occipital lobe					
	Bipolar	0.36±(0.055)			
	Healthy controls	0.32±(0.040)			
			10.66	1,44	0.0021
Inter-hemispheric Efficiency Frontal lobe					
	Bipolar	3.49±(0.46)			
	Healthy controls	3.86±(0.37)			
			15.62	1,44	2.8×10^{-4}
Inter-hemispheric Efficiency Temporal lobe					
	Bipolar	1.60±(0.17)			
	Healthy controls	1.73±(0.21)			
			11.79	1,44	0.0013

Figure 1

Click here to download high resolution image

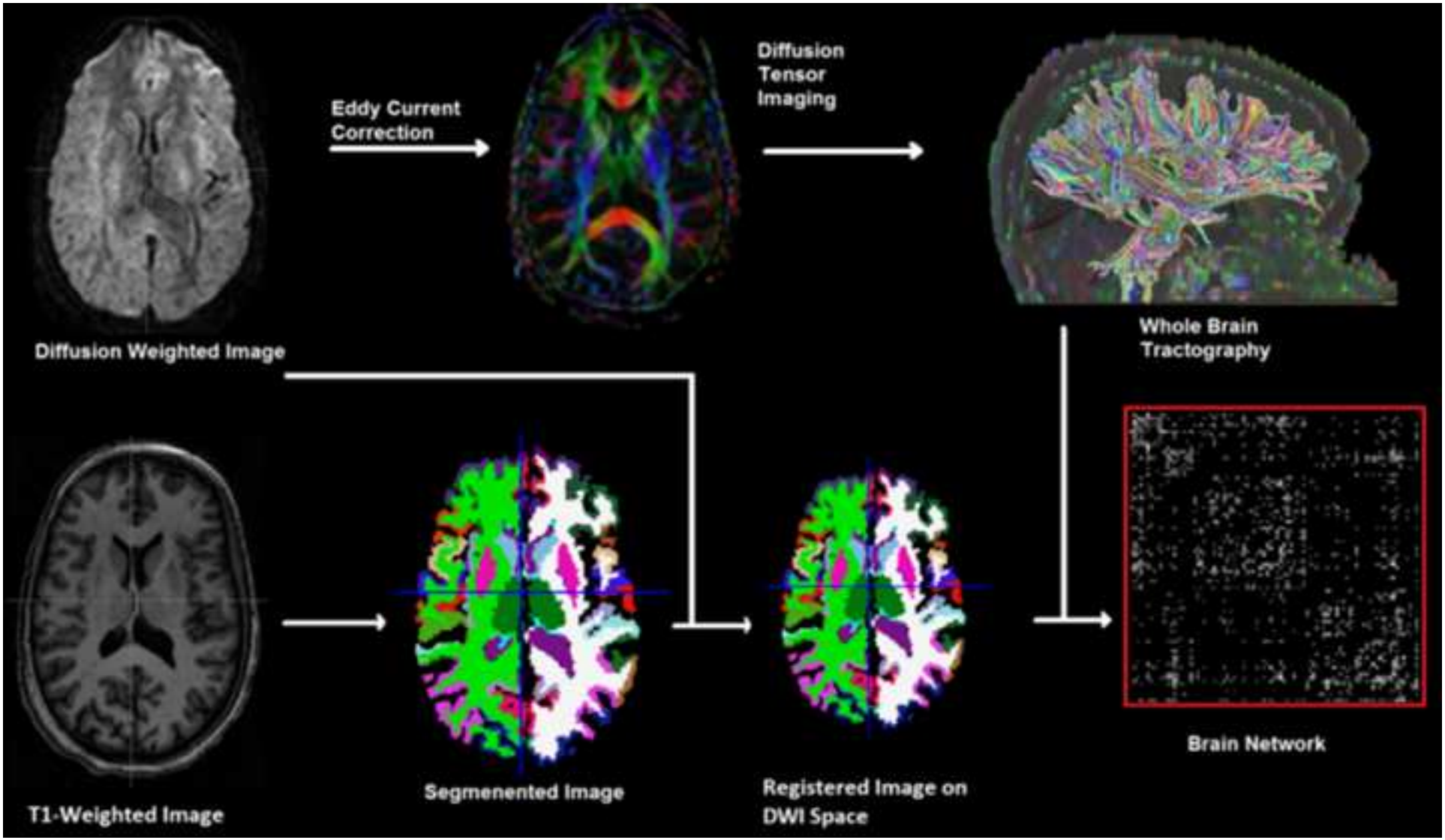

Figure 2

Click here to download high resolution image

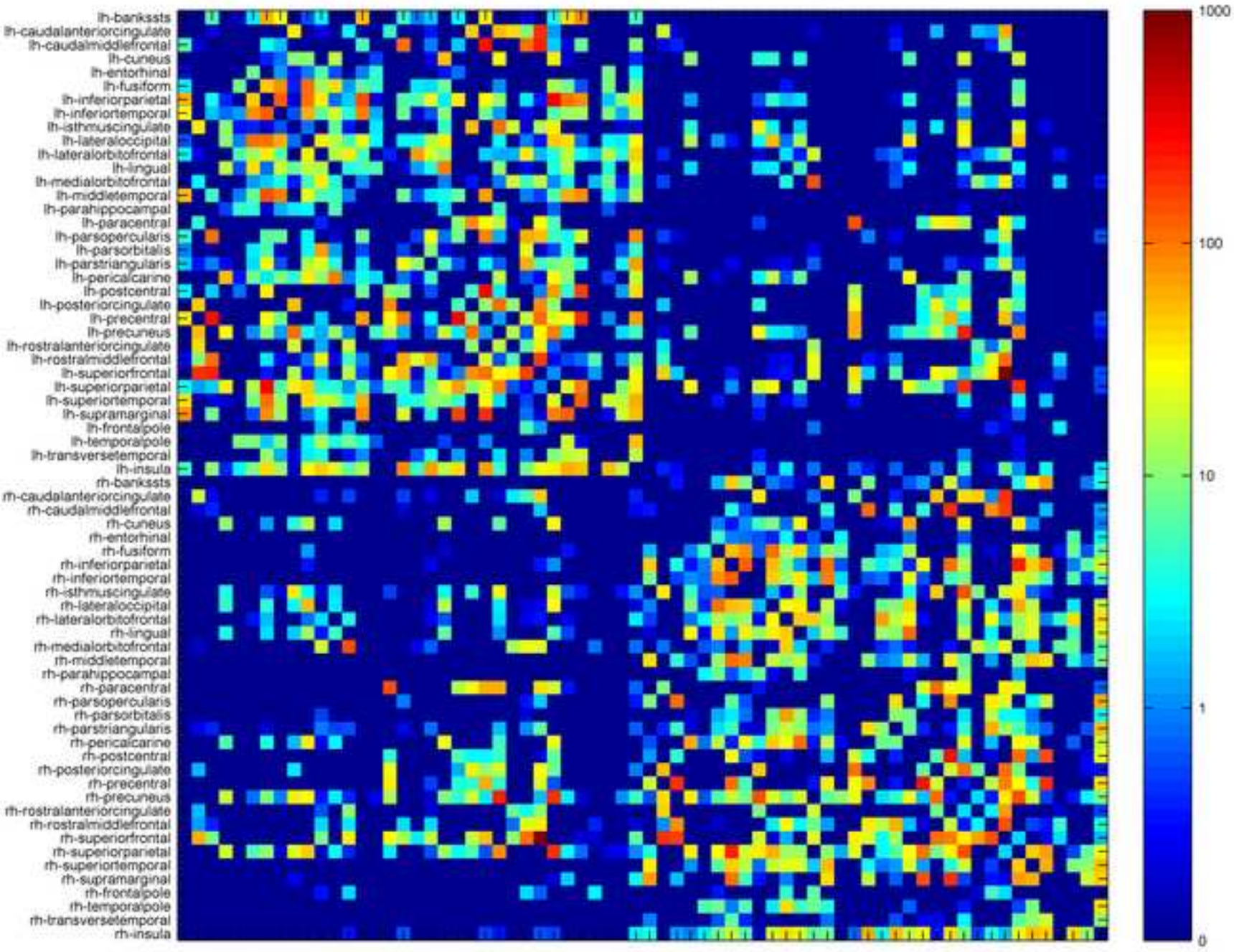

Figure 3

Click here to download high resolution image

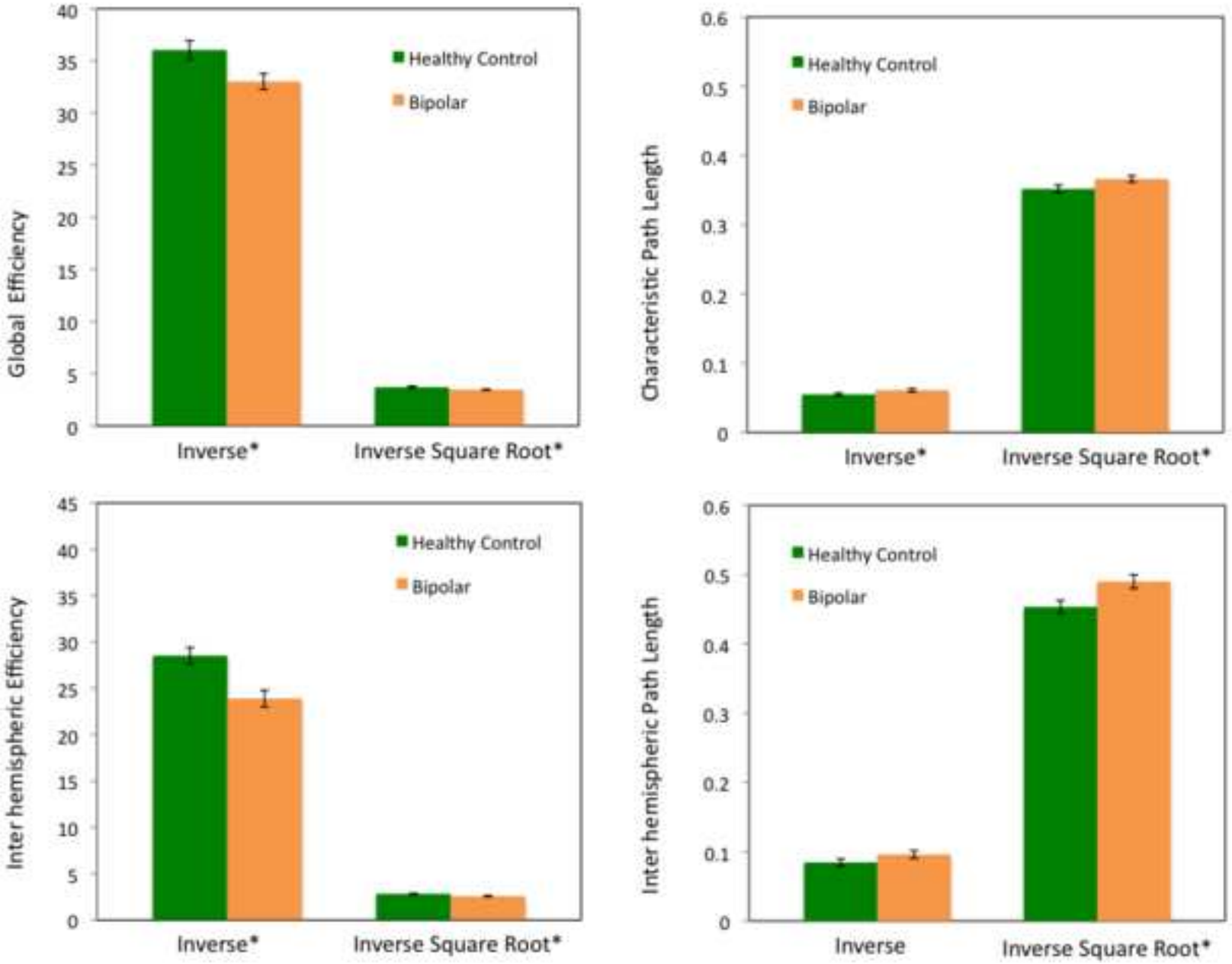

Mathematically, the characteristic path length and global efficiency (CPL and E_{glob}) are defined as:

$$CPL = \frac{\sum_{n,\, m \in N;\; n \neq m} d_{nm}}{\{N\}^2 - \{N\}}$$

$$Eglob = \frac{\sum_{n,\, m \in N;\; n \neq m} d_{nm}^{-1}}{\{N\}^2 - \{N\}}$$

Here, *N* denotes the whole network, {N} the number of nodes in the whole network, and d_{nm} the length of the shortest path connecting nodes n and m.

For the proposed metrics, we defined the intra-modular path length (intra-PL) for module M_i as:

$$\text{intra-PL}^{M_i} = \frac{\sum_{n,\, m \in M_i;\; n \neq m} d_{nm}}{\{M_i\}^2 - \{M_i\}}$$

Here $\{M_i\}$ denotes the number of nodes in module M_i. Similarly, the inter-modular path length (inter-PL) between modules M_i and M_j is mathematically defined as:

$$\text{inter-PL}^{M_i \leftrightarrow M_j} = \frac{\sum_{n \in M_i;\; m \in M_j} d_{nm}}{\{M_i\}\{M_j\}}$$

Lastly, the intra-modular and inter-modular efficiency (E_{intra} and E_{inter}) are mathematically defined as follows.

$$E_{intra}^{M_i} = \frac{\sum_{n,\, m \in M_i;\; n \neq m} d_{nm}^{-1}}{\{M_i\}^2 - \{M_i\}}$$

$$E_{inter}^{M_i \leftrightarrow M_j} = \frac{\sum_{n \in M_i;\; m \in M_j} d_{nm}^{-1}}{\{M_i\}\{M_j\}}$$

Supplemental Figure and Table (will be made online)

Figure S

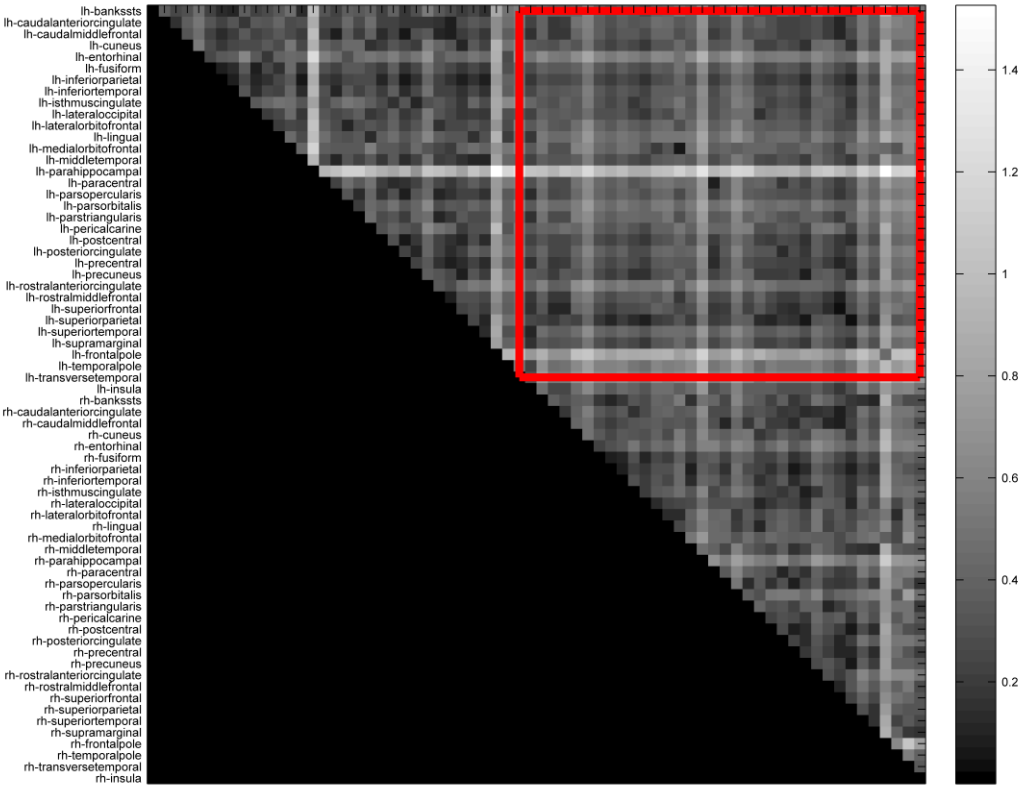

Figure S The brain network distance matrix from a normal control subject in this study. The elements of this matrix indicate the shortest weighted path length connecting node pairs. Only the upper-diagonal part is shown, as the matrix is symmetrical. In this example, the element-wise inverse of the element-wise square root mapping is used. The prefix lh and rh indicate nodes in the left and right hemispheres, respectively. The area outlined in red denotes inter-hemispheric connections.

Table S. Mean and standard deviation (SD) of node-level path lengths for the 20 fronto-limbic ROIs proposed in our a priori hypotheses. Here, node-level path length was computed using the element-wise inverse square root connectivity-to-length mapping. Only regions reaching statistical significance (uncorrected) are shown.

		Path Length	***F***	***df***	***P***
Hippocampus, left					
	Bipolar	0.32±(0.025)			
	Healthy controls	0.30±(0.028)			
			7.926	1,44	0.007
Isthmus cingulate, left					
	Bipolar	0.38±(0.032)			
	Healthy controls	0.35±(0.043)			
			5.467	1,44	0.024
Lateral orbitofrontal, left					
	Bipolar	0.33±(0.025)			
	Healthy controls	0.32±(0.026)			
			13.117	1,44	0.001
Parahippocampal, left					
	Bipolar	0.55±(0.074)			
	Healthy controls	0.49±(0.069)			
			7.979	1,44	0.007
Hippocampus, right					
	Bipolar	0.32±(0.026)			
	Healthy controls	0.31±(0.028)			
			4.717	1,44	0.035
Medial orbitofrontal, right					
	Bipolar	0.37±(0.043)			
	Healthy controls	0.35±(0.029)			
			8.911	1,44	0.005
Isthmus cingulate, right					
	Bipolar	0.34±(0.024)			
	Healthy controls	0.32±(0.035)			
			9.176	1,44	0.004

In this issue statement

We acquired diffusion-weighted MRI on 25 bipolar I subjects and 24 gender and age equivalent healthy controls. We investigated white matter integrity in the whole brain, and conducted first ever brain network analyses in bipolar disorder using a graph-theoretical approach.

Our results revealed that bipolar brain networks exhibited lower local clustering and global efficiency relative to those of controls. Further analyses suggested significantly impaired inter-hemispheric integration in the bipolar group.